Received Signal Interpolation for Context Discovery in Cognitive Radio

Liliana Bolea, Jordi Pérez-Romero, Ramon Agustí
Dept. of Signal Theory and Communications (TSC)
Universitat Politècnica de Catalunya (UPC), Barcelona, Spain
Email : [lilianab, jorperez, ramon]@tsc.upc.edu

Abstract— **This paper addresses the context acquisition to characterize different features of a primary network based on the power measurements obtained by a sensor network. In particular, it presents a comparative study of the impact of natural neighbor, linear, and nearest neighbor interpolation techniques carried out over the measurements at different geographical positions. Extracted features include transmitter position, antenna pattern or propagation model. An evaluation is carried out in scenarios including the effect of both correlated and non-correlated shadowing.**

Keywords-: dynamic spectrum access; radio environment map; interpolation; nearest neighbor; natural neighbor.

I. INTRODUCTION

As it is nowadays widely recognized, the licensed radio frequency spectrum is severely underutilized in most regions [1][2]. As a result, Cognitive Radio (CR) and Dynamic Spectrum Access paradigms [3][4]have emerged in the last decade as a promising solution to exploit the existence of the non used spectrum, the so-called white spaces, through opportunistic spectrum access. It consists in allowing secondary users (SUs) to access in an opportunistic and non-interfering manner some licensed bands temporarily unoccupied by primary users (PUs) holding a license. This primary-secondary spectrum sharing can take the form of cooperation or coexistence, meaning that either there is an explicit communication and coordination between primary and secondary systems, in case of cooperation, or there is none, in case of coexistence [5]. As long as sharing is based on coexistence, secondary devices are essentially invisible to the PUs. Therefore, the complexity of sharing is borne by the SUs and no changes to the primary system are needed.

The decisions that SUs have to take, like the selection of the appropriate spectrum band to transmit, modulation formats, power level, etc., are considerably dependent on the environment and the PUs activity. Most studies are mainly based on the determination of the presence or absence of PUs in the scenario where SUs are to be deployed. However, just knowing whether or not there exists a PU in a particular frequency band is not enough information. A proper estimation of context is essential for an efficient operation of CR networks. This context includes features such as path loss model, transmitter positions, radiation pattern, transmission power and shadowing characterization among others. Once acquired, such rich context information should be stored in a database system, locally or globally, usually denoted as Radio Environment Map (REM) [6] to be used during the secondary network operation.

Not so many published works have tried to characterize the context where a secondary network operates [7][8]. In this respect, [7] is so far one of the most relevant references in terms of a wide context acquisition. It proposes a context characterization algorithm which identifies the presence, positions, and antenna patterns of PUs in a scenario populated by CR nodes acting as sensors and cooperating in a noisy environment. To this end, the Received Signal Strength (RSS) obtained at each receiving sensor and their locations are required. However, it makes the assumption of Gaussian antenna pattern. Furthermore, the complexity of the algorithm is large since it requires either a 3D or 2D search over a set of different parameters.

In this context, the goal of this paper is to explore the characterization of the relevant PUs context features through the use of a simple methodology but still retaining satisfactory performance and without making any a priori considerations regarding the radiation patterns of the PUs. Furthermore, the effects of correlated shadow fading are considered in the deployed area under study. These realistic assumptions make more difficult to face an analytical solution to the problem so a heuristic approach has been retained. In the considered scenario, a number of RF sensors are randomly located in the whole area where the SU network is deployed, and an interpolation mechanism is used to build a suitable estimated RF signal power map from which the different context features are extracted. To this end, the proposed algorithm, based on image processing techniques, expands prior work of the authors in [9] that used nearest neighbor interpolation in the methodology by considering two other interpolation methods, namely linear and natural neighbor interpolation. These two methods, in spite of not retaining the great simplicity of the nearest neighbor interpolation, are still non-involved methodologies that can offer a better characterization of the RF environment. The linear interpolation was first introduced in [10]. In turn, natural neighbor interpolation was suggested by Sibson in [11][12] for data approximation and smoothing. Under these considerations, this paper will present a realistic performance comparison of the above mentioned interpolation approaches when used in a typical deployment scenario, comparing also the effect of non-correlated and correlated shadow fading.

The rest of the paper is organized as follows. Section II presents in more detail the system model and problem that is considered in this paper, while Section III describes the proposed methodology with particular focus on the interpolation methods. Section IV presents performance results under different conditions, and finally, Section V summarizes the conclusions.

II. Scenario Consideration and Problem Formulation

A generic scenario is considered, which is characterized by a number of primary transmitters that operate at different frequencies and have different coverage areas. A secondary network will rely on the information measured by a number of sensors, which are randomly distributed in the scenario, and also on the appropriate post-processing of this information, in order to estimate different context parameters of the primary network. The results could be stored in a REM, for further assistance in future decisions of the secondary network operation. It is assumed that sensors cooperate with each other in a centralized manner, where a central entity gathers all information from the sensors and estimates the context parameters. Having this information, the central entity would analyze the characteristics of the radio environment, in particular the detected spectrum holes, and assign the appropriate frequencies to the SU terminals.

A sensor measures the RSS in a number of frequencies in its geographical position. It is assumed that frequency f_i is detected by the sensor at position (x,y) when the received power RSS is above a given threshold $P_{th}(f_i)$. The value detected by a sensor for each frequency is quantified to a set of 2^n values with quantization step Δ. Then, this value will be encoded as a word of n bits and sent to the central entity.

Different RSS measurements at random positions associated to the sensors represent a partial vision of the scenario. The problem considered here consists in defining a methodology to smartly combine these measurements in order to get a full vision in which the primary transmitter networks are estimated. This work focuses mainly on this combination of the sensing results, assuming these results are available. Both the considerations on the sensing process itself (such as errors in the process or the determination of which frequencies has to measure every sensor) and the means to report the sensing results are out of the scope of the paper.

III. Problem Methodology

The proposed methodology assumes that the radio environment can be characterized by an image [13], where each pixel (i.e., a rectangular area of dimensions $\Delta x \times \Delta y$) contains the information of the RSS levels associated to the frequencies measured in this area. It is assumed that a pixel can only have the result of one sensor. Then, given that only the values of the pixels where a sensor is located are known, these values need to be combined using image processing techniques in order to reconstruct the overall image and to discover the following context features: transmitter positions, orientations of their directional antennas, radiation pattern, and propagation model.

The steps of the proposed methodology are illustrated in Fig. 1 and explained in the following, with a particular focus on the interpolation process that constitutes the difference with respect to prior work of the authors in [9].

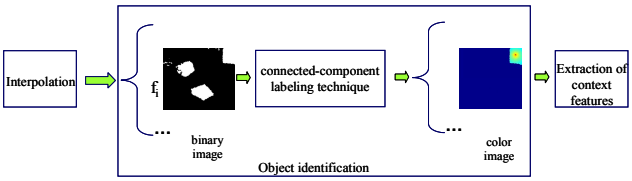

Figure 1. Overall steps of the methodology.

A. Interpolation

Interpolation is the process of determining the value of a function between two or more points at which it has prescribed values (i.e., the sensor positions). This is the first step intended to determine the RSS associated to those pixels without any sensor based on the pixels available. As was mentioned before, three methods of interpolation are used.

1) Nearest neighbor interpolation: In this method the value of the unknown pixel $P(x,y)$ is interpolated as:

$$P(x,y) = \min_{d_k} P_k(x_k, y_k) \quad (1)$$

that is, the value of $P(x, y)$ is simply obtained as the value measured by the closest sensor (i.e., the one with minimum distance d_k). This algorithm is very simple to implement.

2) Linear interpolation: It involves estimating a new value by connecting two adjacent known values with a straight line. If the two known values are $P_1(x_1, y_1)$ and $P_2(x_2, y_2)$, then the interpolated value at position (x, y) is:

$$P(x,y) = P_1(x_1,y_1) + u\left(P_2(x_2,y_2) - P_1(x_1,y_1)\right) \quad (2)$$

where u is a number between 0 and 1 representing the fraction of the distance between (x_1, y_1) and (x_2, y_2) at which (x, y) lies. This method works best when the function is not changing quickly between known values.

3) Natural neighbor interpolation: It is a weighted average method that constructs the interpolant by using natural neighbor coordinates based on Voronoi tessellation of a set of positions. This has the advantage over simpler methods in that it provides a smoother approximation to the underlying "true" function. Interpolation is given by the following expression:

$$P(x,y) = \sum_{k=1}^{n} f_k(x,y) \cdot P(x_k, y_k) \quad (3)$$

where (x,y) is the query point to be interpolated, and $P(x,y)$ is the corresponding interpolated function value at this query point, [11][12]. The points (x_1, y_1), (x_2, y_2), …,(x_k, y_k) are the k natural neighbors of the query point (x, y) in the Voronoi diagram of the original data sites, with known function values at each point, $P(x_1, y_1)$, $P(x_2, y_2)$, …, $P(x_k, y_k)$. The values $f_1(x, y)$, $f_2(x, y)$, …, $f_k(x, y)$ are the coefficients for each neighboring point of the query point, and are referred to as natural neighbor

coordinates for each natural neighbor point. Fig. 2 shows a 2D example, where query point *(x,y)* has 5 natural neighbors (x_1,y_1), …, (x_5,y_5).

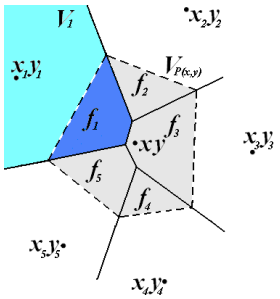

Figure 2. Natural neighbor coordinates in 2D.

The area labeled $f_1(x,y)$ is the overlap between the Voronoi polygon associated with the query point *(x,y)*, $V_{P(x,y)}$, and the Voronoi polygon associated with the data (x_1,y_1), V_1. Then the natural neighbor coordinate of *(x,y)* with respect to (x_1,y_1) is the ratio of the area of the dark blue polygon over the area of the total highlighted zone in grey, $V_{P(x,y)}$.

$$f_1(x,y) = \frac{Area\left(V_{P(x,y)} \cap V_1\right)}{Area\left(V_{P(x,y)}\right)} \tag{4}$$

B. Object identification

In this step, the target is the identification of the different transmitters existing in the scenario. This is done under the assumption that the area where a transmitter at frequency f_i is being detected can be considered as an "object" inside the image, so object identification techniques are applied. As shown in Fig. 1, the following steps are carried out.

- From the resulting interpolated image, a set of binary images is built, one per frequency f_i. Each pixel of a binary image takes the value 1 if frequency f_i, is detected (i.e., it is above $P_{th}(f_i)$) and 0 otherwise. These images will be used as the basis to identify the different "objects".

- For each binary image, an object identification mechanism following the so-called connected-component labeling technique [14] is applied. It consists in scanning the image and making groups of adjacent pixels having the same value (it is assumed that two pixels are adjacent if they have one of their 4 edges in common). Each group of pixels will be then an "object".

- Next, the binary images are converted into color images, one per each object identified, using the quantified values from the received power at each frequency f_i after the interpolation.

C. Extraction of context features

For each of the objects identified in the previous step a set of context features are extracted following a procedure composed of four steps, namely transmitter position estimation, antenna orientation estimation, antenna pattern radiation estimation, and propagation model estimation. A detailed and in-depth description of the operations performed in each step can be found in [9].

IV. RESULTS

This section evaluates the proposed methodology in a scenario with a transmitter equipped with a directive antenna. Scenario size is 3780 m x 3780 m with pixel size $\Delta x = \Delta y = 20$ m. The EIRP is 55 dBm, and power threshold $P_{th}(f_i)$ is -85 dBm. The number of bits used to encode the RSS measurements is $n = 5$ bits, and the quantization step is $\Delta = 1.5$ dB. Based on the propagation model used in the area of the transmitter, the expected received power in dBm at distance *d(m)* should be:

$$P = P_0 - 10\alpha \log(d) + S \tag{5}$$

where $P_0 = 24.5$ dBm is received power at 1 m, $\alpha = 3.552$ is the path loss exponent, and S is a Gaussian random variable with mean 0 and standard deviation σ (dB) representing the shadowing losses.

Three different situations are analyzed, considering first the case where no shadowing exists, and then the cases with non-correlated and spatially correlated shadowing.

A. Case without shadowing

Fig. 3 presents the mean error and standard deviation (vertical lines) of the transmitter position (a) and antenna direction estimation (b), respectively, for different values of sensor density D, for all three methods of interpolation in the absence of shadowing losses in the received power. Results were averaged over 150 realizations of the sensors distribution. For a low sensor density such as D = 4 sensors/km^2 the mean error as well as the standard deviation error in both position estimation and antenna direction estimation are high for all three interpolation methods. As the density of sensors grows, errors are reduced. For example, with 50 sensors/km^2 the error is roughly 80 m that corresponds to 4 pixels. As a reference, this is approximately 5% of the transmitter coverage radius in the direction of the maximum antenna gain. All the three methods present a very similar behavior.

Concerning the estimation of the propagation model, Fig. 4 presents the mean error and standard deviation error (vertical lines) of the propagation factor α in Fig. 4 (a), respectively power P_0 in Fig. 4 (b), as functions of sensor density D. Also the theoretical values according to (5) are plotted. Errors with respect to these theoretical values reduce when increasing the sensor density. For both parameters, natural neighbor and linear interpolation give a lower standard deviation error than nearest neighbor. It can be noted that neither in the estimation of the position nor of the propagation model parameters there exists a significant gain when the sensor density increases above 50 sensors/km^2, approximately.

The estimated radiation pattern of the primary transmitter antenna is presented in Fig. 5 for the case D = 50 sensors/km^2, for all three methods of interpolation, and their standard deviation error is presented in TABLE I. It can be noticed how the estimated radiation patterns follow quite adequately the original radiation pattern, particularly in the main lobe, and differences with respect to the real pattern mainly appear in the back side of the antenna. In this case, natural neighbor interpolation and linear interpolation perform very similarly

and both offer better results than nearest neighbor. A slightly lower standard deviation error is given by linear interpolation as seen in TABLE I.

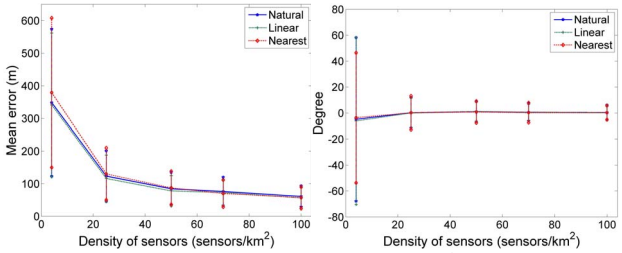

a. b.

Figure 3. Mean error and standard deviation in transmitter position estimation (a) and in antenna direction estimation (b), for different sensor densities, case without shadowing.

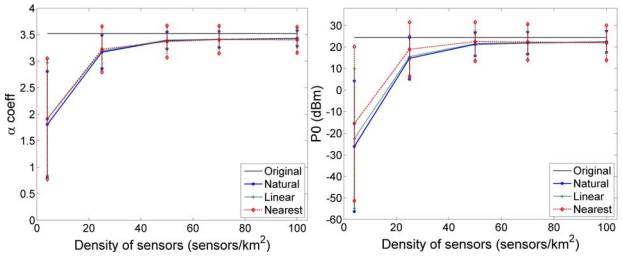

a. b.

Figure 4. Estimated propagation factor α (a) and estimated P_0 (b), as a function of the sensor density, case without shadowing

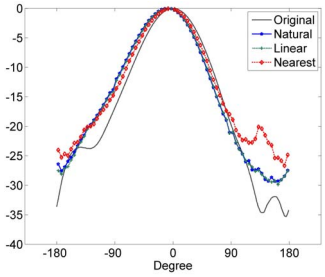

Figure 5. Horizontal radiation pattern of primary transmitter's antenna, for the case D = 50 sensors/km^2, case without shadowing.

TABLE I. STANDARD DEVIATION IN HORIZONTAL ANTENNA RADIATION PATTERN FOR THE CASE D = 50 SENSORS/KM^2, CASE WITHOUT SHADOWING

	Natural	***Linear***	***Nearest***
Standard Deviation (dB)	4.0763	4.0574	8.4599

B. Scenario with non-correlated shadowing

In this section, random shadowing losses are added to the original scenario with a standard deviation σ = 6 dB. Non-correlated shadowing is considered first, meaning that the shadowing losses are independent in all the pixels of the scenario. Fig. 6 (a) presents the mean error and standard deviation error (vertical lines) of the position estimation, for different values of sensor density D, for all three methods of interpolation. Similarly, Fig. 6 (b) presents the mean error and standard deviation error in the antenna's direction estimation. Like in the previous sub-section, results were averaged over 150 realizations of sensors distribution. As expected, errors are reduced as the density of sensors increases. The performance is approximately the same with all three considered methods. When comparing with the case without shadowing in Fig. 3 it can be observed how the introduction of shadowing causes an increase in the estimation errors and the standard deviations.

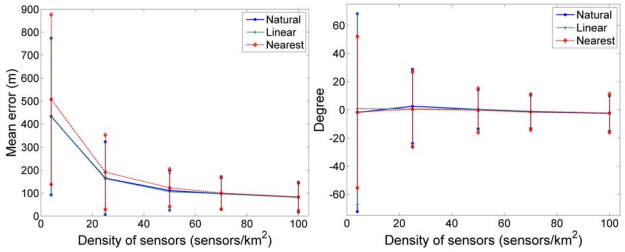

a. b.

Figure 6. Mean error and standard deviation in transmitter position estimation (a) and in antenna direction estimation (b), for different sensor densities, non-correlated shadowing.

Fig. 7 shows the corresponding results for the mean error and standard deviation error of the propagation factor α and power P_0 for different values of sensor density D. Errors are reduced as the density of sensors increases. In this case, it can be observed how the nearest neighbor case offers the worst performance among the considered interpolation methods, while the differences between the natural neighbor and linear cases are small. A similar conclusion is observed in TABLE II that presents the standard deviation error of the estimated antenna radiation pattern for the case D = 50 sensors/km^2. Nearest neighbor exhibits the largest deviation in the error, while the performance of linear and natural neighbor cases is very similar.

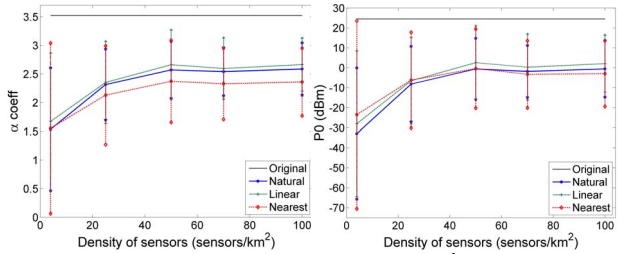

a. b.

Figure 7. Estimated propagation factor α (a) and estimated P_0 (b), as a function of the sensor density, non-correlated shadowing..

TABLE II. STANDARD DEVIATION IN HORIZONTAL ANTENNA RADIATION PATTERN, FOR THE CASE D = 50 SENSORS/KM^2, NON-CORRELATED SHADOWING

	Natural	***Linear***	***Nearest***
Standard Deviation (dB)	5.4945	6.1667	11.449

C. Scenario with correlated shadowing

In this part, correlated shadowing losses with 6 dB shadowing standard deviation are added to the original scenario. Shadowing is spatially correlated following an exponential autocorrelation function with decorrelation distance *dcorr* = 400 m. The generation of 2D spatially correlated shadowing is done using the methodology of [15]

based on filtering a set of independent shadowing samples using a 2D filter defined from the Fourier transform of the exponential autocorrelation function. Results are obtained by averaging a total of 10 different shadowing realizations of the scenario, each of them consisting in turn in 150 realizations of the sensor distribution. TABLE III shows the simulation results, for the case D = 50 sensors/km^2, for all three methods of interpolation, and comparing them with the cases without shadowing and non-correlated shadowing. Results are presented in terms of the average and standard deviation values of the error in the position, the antenna direction, and the propagation model parameters. It can be observed how the case of correlated shadowing in general exhibits better estimation errors than the case of non-correlated shadowing for all parameters with the only exception of the antenna direction. In general, linear and natural neighbor interpolations present better results than the nearest neighbor. Differences are particularly significant from the perspective of standard deviation, which is larger with the nearest neighbor interpolation.

TABLE III. SIMULATION RESULTS, FOR THE CASE D = 50 SENSORS/KM^2

	Pos. error -Avg (m)	Pos. error –Std. dev (m)	Dir. error -Avg (º)	Dir. error – Std. dev (º)	α (avg)	α (Std. dev)	P_0 - Avg (dBm)	P_0 – Std. dev (dB)
	Natural neighbor interpolation							
No sdw	84.5	50.5	1.02	7.71	3.39	0.16	21.6	5.4
Non corr. sdw	111	86.2	0.21	13.8	2.57	0.49	-0.54	15.3
Corr sdw	99.9	69.0	3.83	9.31	2.74	0.32	6.13	10.3
	Linear interpolation							
No sdw	78.0	46.7	1.04	7.35	3.40	0.16	21.9	5.62
Non corr. sdw	105	79.9	0.30	13.9	2.66	0.60	2.57	18.3
Corr sdw	93.2	63.9	4.03	9.20	2.79	0.33	7.62	10.6
	Nearest neighbor interpolation							
No sdw	87.3	51.1	0.75	8.37	3.38	0.30	23.4	9.13
Non corr. sdw	123	81.5	-0.41	15.6	2.37	0.71	-0.34	19.8
Corr sdw	98.6	66.8	4.40	10.2	2.84	0.48	12.0	14.6

V. CONCLUSIONS

This paper has presented a comparative study of the natural neighbor, linear, and nearest neighbor interpolation techniques used to combine a set of radio signal strength measurements obtained by a sensor network. Proposed methodology targets the estimation and characterization of different context features such as transmitter position, antenna pattern estimation and propagation model characterization. Results have been analyzed in different situations depending on the type of shadowing losses in the environment. It has been inferred that, in absence of shadowing, the proposed methodology is able to extract the transmitter position, the antenna pattern, and propagation model features adequately regardless the considered interpolation technique. On the other hand, when shadowing is present, either spatially correlated or non-correlated, the errors increase. In this case, nearest neighbor interpolation provides similar performance from an average perspective but exhibits a larger dispersion than natural neighbor and linear interpolation depending on how sensors are located in the different realizations.

ACKNOWLEDGMENT

This work was supported by the European Commission in the framework of the FP7 FARAMIR Project (Ref. ICT-248351) and by the Spanish Research Council and FEDER funds under ARCO grant (ref. TEC2010-15198). The support from the Spanish Ministry of Science and Innovation (MICINN) under FPU grant AP2008-02291 is also hereby acknowledged.

REFERENCES

[1] F. C. Commission, “Spectrum policy task force,” Rep. ET Docket vol. 02-135, 2002.

[2] T.X. Brown, “An analysis of unlicensed device operation in licensed broadcast service bands,” IEEE DySPAN, pp. 11 – 29, Nov. 2005.

[3] J. Mitola, III and G. Q. Maguire, Jr., “Cognitive radio: making software radios more personal,” Personal Communications, IEEE, vol. 6, pp. 13 – 18, 1999.

[4] S. Haykin, “Cognitive radio: brain-empowered wireless communications,” Selected Areas in Communications, IEEE Journal on, vol. 23, pp. 201 – 220, 2005.

[5] V. Petty et at, “Feasibility of dynamic spectrum access in underutilized television bands,” IEEE DySPAN, pp. 331 – 339, Apr. 2007.

[6] Y. Zhao, L. Morales, J. Gaeddert, K. K. Bae, J.-S. Um, and J. H. Reed, “Applying radio environment maps to cognitive wireless regional area networks,” IEEE DySPAN, pp. 115 – 118, April 2007.

[7] R. K. Martin and R. Thomas, “Algorithms and bounds for estimating location, directionality, and environmental parameters of primary spectrum users,” Wireless Communications, IEEE Transactions on, vol. 8, no. 11, pp. 5692 – 5701, Nov. 2009.

[8] A. A. Honoré, R. W. Thomas, R. K. Martin, and S. H. Kurkowski, “Implementation of collaborative rf localization using a software-defined radio network,” IEEE MILCOM, pp. 1 – 7, Oct. 2009.

[9] L. Bolea, J. Pérez-Romero, R. Agustí, and O. Sallent, “Context discovery mechanisms for cognitive radio”, IEEE VTC 2011 Spring, May 2011, in press.

[10] H. Gouraud, “Continuous shading of curved surfaces,” IEEE Transactions on Computers, 20(6), pp. 623 – 629, 1971.

[11] R. Sibson, “A vector identity for the dirichlet tesselation,” In Mathematical Proceedings of the Cambridge Philosophical Society, 87, pp. 151 – 155, 1980.

[12] R. Sibson, “A brief description of natural neighbor interpolation,” In V. Barnett, editor, Interpreting Multivariate Data, pp. 21 – 36, 1981.

[13] J. Pérez-Romero, O. Sallent, R. Agustí, “On the applicability of image processing techniques in the radio environment characterisation,” IEEE VTC 2009 Spring, pp. 1 – 5, Apr. 2009.

[14] R. Fisher, S. Perkins, A. Walker and E. Wolfart (2003) “Connected component labeling,” Available at: http://homepages.inf.ed.ac.uk/rbf/HIPR2/label.htm#1, May 2011.

[15] R. Fraile, J. Gozálvez, O. Lázaro, J. Monserrat, and N. Cardona “Effect of a two dimensional shadowing model on system level performance evaluation”, WPMC, vol. 2, pp. 149 – 153, Sept. 2004.